

Direct Synthesis of Chromium Perovskite Oxyhydride with a High Magnetic-Transition Temperature**

Cédric Tassel, Yoshihiro Goto, Yoshinori Kuno, James Hester, Mark Green, Yoji Kobayashi, and Hiroshi Kageyama*

Abstract: We report a novel oxyhydride SrCrO_2H directly synthesized by a high-pressure high-temperature method. Powder neutron and synchrotron X-ray diffraction revealed that this compound adopts the ideal cubic perovskite structure ($\text{Pm}\bar{3}\text{m}$) with O^{2-}/H^- disorder. Surprisingly, despite the non-bonding nature between $\text{Cr } 3d$ t_{2g} orbitals and the $\text{H } 1s$ orbital, it exhibits G-type spin ordering at $T_N \approx 380$ K, which is higher than that of RCrO_3 (R = rare earth) and any chromium oxides. The enhanced T_N in SrCrO_2H with four Cr-O-Cr bonds in comparison with $\text{RCr}^{3+}\text{O}_3$ with six Cr-O-Cr bonds is reasonably explained by the tolerance factor. The present result offers an effective strategy to tune octahedral tilting in perovskites and to improve physical and chemical properties through mixed anion chemistry.

Oxide perovskites ABO_3 are the most encountered compounds in solid-state chemistry. Their compositional flexibility allows numerous properties often establishing ground-breaking performances in applied devices, such as colossal magneto-resistivity,^[1] dielectrics,^[2] and high-temperature superconductivity.^[3] However, increasing attention has been paid to mixed-anion perovskites, such as oxyfluorides ABO_2F and oxynitrides ABO_2N as promising alternative materials in pigments,^[4] water-splitting photocatalysis,^[5] dielectric properties,^[6]

and cathode material.^[7] Their properties arise from the substitution of oxygen with other anions as well as the fine tuning of the anionic and interacting d bands of the octahedral center B.

Unlike the 2p based anions O^{2-} , F^- , S^{2-} , N^{3-} , the hydride H^- anion is unique and only has a filled $1s^2$ shell. Its combination with a 2p anion as well as its interactions with the B element could be very interesting towards developing novel magnetic and transport properties. However, preparation of

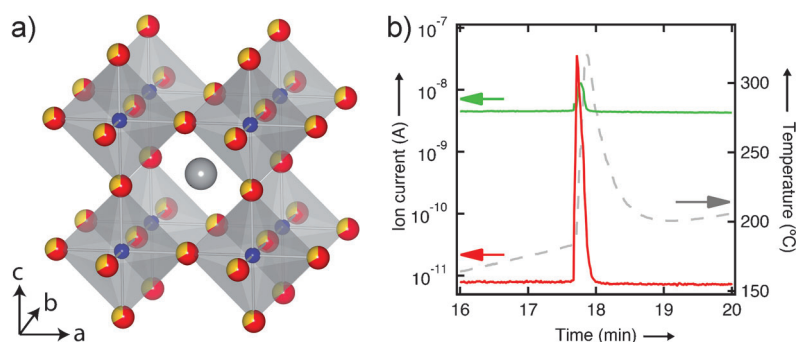


Figure 1. a) Crystal structure of SrCrO_2H with cubic perovskite structure ($\text{Pm}\bar{3}\text{m}$). Gray strontium, blue chromium, and red/gold anion (oxide/hydride) sites. b) Mass spectrometry of H_2 desorption (red) during oxidation of SrCrO_2H in flowing oxygen. A small peak derived from H_2O (green) was also observed. The dotted line plots the temperature at the sample, where the rapid increase indicates the exothermic reaction upon H_2 release/ O_2 uptake.

[*] Dr. C. Tassel, Y. Goto, Y. Kuno, Dr. Y. Kobayashi, Prof. H. Kageyama
Graduate School of Engineering, Kyoto University
Kyoto 615-8510 (Japan)
E-mail: kage@scl.kyoto-u.ac.jp

Dr. C. Tassel
The Hakubi Center for Advanced Research, Kyoto University
Kyoto (Japan)

Dr. J. Hester
Bragg Institute, Australian Nuclear Science and Technology
Organization (ANSTO)
Locked Bag 2001, Kirrawee DC NSW 2232 (Australia)

Prof. M. Green
NIST Center for Neutron Research, National Institute of Standards
and Technology
100 Bureau Drive, MS 6100, Gaithersburg (USA)

[**] This work was supported by the Hakubi Project funding, MEXT
through Grant-in-Aid for Scientific Research A (No. 24248016) and
the Young Scientist Grant B (No. 25810040) and JSPS through
FIRST Program and CREST.

Supporting information for this article is available on the WWW
under <http://dx.doi.org/10.1002/ange.201405453>.

oxyhydrides has been a significant challenge, mainly because hydride itself is a strong reducing agent. LaHO and $\text{Ba}_{21}\text{Ge}_2\text{O}_5\text{H}_{24}$ were prepared by solid-state reaction in vacuum,^[8] while $\text{FeAsLa}(\text{O},\text{H})$ superconductors were prepared under high pressure.^[9] Topochemical reactions were employed to yield layered perovskite oxyhydrides $\text{LaSrCoO}_3\text{H}_{0.7}$ and $\text{Sr}_3\text{Co}_2\text{O}_{4.33}\text{H}_{0.84}$ using CaH_2 as a reductant.^[10]

There has been only one oxyhydride perovskite reported to date, $\text{BaTiO}_{3-x}\text{H}_x$ that can be prepared through the low-temperature hydride reduction of BaTiO_3 .^[11] $\text{BaTiO}_{3-x}\text{H}_x$ is non-stoichiometric, with hydride substitutable up to $x=0.6$. Similar reactions with iron or nickel perovskite oxides did not afford the insertion of hydride, although the products are highly oxygen deficient (SrFeO_2 , LaNiO_2).^[12] Herein, we show a stoichiometric oxyhydride perovskite SrCrO_2H (Figure 1) synthesized using a high-pressure high-temperature technique. This material is the first chromium oxyhydride. We also found that neighboring Cr^{3+} spins order antiferromagnetically at high temperature ($T_N \approx 380$ K), which is rather surprising given the non-bonding nature of

Cr–H bonds between Cr 3d t_{2g} and H 1s orbitals. The observed properties are discussed in comparison with the related $RCr^{3+}O_3$ family (R = rare earth) that exhibits a spin order at much lower temperatures.

In recent years, high-pressure synthesis has been widely used in the synthesis of transition-metal hydrides: binary systems (e.g., FeH) as well as ternary $LiNiH_3$ and $CaPdH_3$ adopting the perovskite structure.^[13] The formation of complex metal hydrides usually requires synthesis temperatures that are far beyond the decomposition temperatures of the hydride precursors. While high temperature might favor decomposition of hydrides in the equilibrium of “metal + H_2 = metal hydride”, high external and high hydrogen pressure will stabilize a solid hydride with a dense structure.

The high-pressure and high-temperature reaction technique was therefore chosen as a pathway to yield an oxyhydride perovskite $SrCrO_2H$ with a dense structure while preventing its decomposition during heating. This composition with Cr in a trivalent state was selected because of its stability against reduction; no binary intermediate phase exists between Cr and Cr_2O_3 .^[14] The best quality was achieved when the stoichiometric mixture of SrH_2 , SrO , and Cr_2O_3 was heated at 5 GPa and 1000 °C, yielding a cubic phase with $a \approx 3.83441(2)$ Å. Lower pressures and temperatures resulted in low-purity samples containing residual precursors. Higher temperature reactions led to the reaction of Cr_2O_3 with the NaCl sleeve to give $NaCr_2O_4$. Note that attempts to topotactically obtain the target oxyhydride from $SrCrO_3$ were unsuccessful; as previously reported, the CaH_2 reaction of $SrCrO_3$ gave oxygen-deficient phases of $SrCrO_{2.75}$ and $SrCrO_{2.8}$.^[15]

To confirm the presence of hydrogen in our sample, we monitored, using a mass spectrometer, desorbed gases upon heating under oxygen flow ($10^\circ C min^{-1}$). Figure 1b shows a sharp H_2 peak ($n=2$) at around 170 °C together with a smaller peak associated with H_2O , indicative of a significant amount of hydrogen in the specimen. After this experiment, the sample was studied by X-ray diffraction (XRD), revealing a mixture of oxidized $SrCrO_4$ and $SrCrO_3$.

Synchrotron powder X-ray diffraction (SPXRD) profile (Figure 2a) was indexed with a primitive cubic structure. The obtained lattice parameter of $a = 3.83441(2)$ Å is slightly longer than that of $SrCrO_3$ ($a = 3.818$ Å).^[16] A few unknown peaks not visible in the laboratory XRD were observed. Rietveld structural analysis was performed using the cubic perovskite model ($Pm\bar{3}m$), with Sr placed on 1b (0.5, 0.5, 0.5), Cr on 1a (0, 0, 0) and O^{2-} on 3d (0.5, 0, 0). Hydrogen is too light to be observed by XRD and thus is not considered here. The refinement readily converged to reasonable agreement parameters of $R_{wp} = 8.45\%$ and $GOF = 3.85$. The oxygen site occupancy (g_O) of 0.6699(4) indicates a nearly stoichiometric composition of $SrCrO_{2.009(1)}$. No off-stoichiometry was found in both cationic sites. Transmission electron microscopy experiments at room temperature demonstrate diffraction patterns compatible with a simple cubic perovskite (see the inset of Figure 2a). The energy dispersive X-ray spectrometry (EDS) confirmed the cation ratio of Sr/Cr = 1.

Neutron powder diffraction (NPD) profile at room temperature (Figure 2b and Figure S1) exhibits, in addition

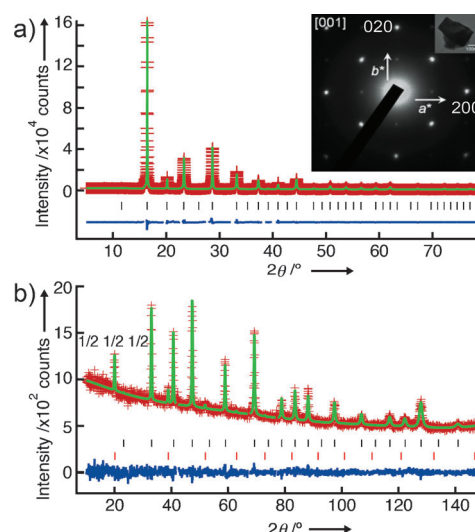


Figure 2. Structural characterization of $SrCrO_2H$ by Rietveld refinement of SPXRD at 290 K (a) and NPD at 300 K (b). The inset in (a) shows an electron diffraction pattern of $SrCrO_2H$ taken along [001]. Red crosses = observed, green solid line = calculated, and blue solid line = difference intensities. Black dashes = calculated Bragg reflections and red dashes = magnetic reflections. A few angle ranges contained tiny peaks from an unknown impurity and were excluded from the fit.

to nuclear peaks, magnetic peaks that are indexed with a propagation vector (π, π, π ; see below). Rietveld analysis on the basis of the O/H disordered model confirmed the presence of hydrogen located at the 3d Wyckoff position with the refined occupancy of $g_O = 0.337(2)$, along with good agreement parameters of $R_{wp} = 3.85\%$ and $GOF = 0.96$. Note that the model without hydrogen resulted in an unrealistic stoichiometry of $SrCrO_{1.338(9)}$ having $Cr^{0.7+}$. No off-stoichiometry was again found in both cationic sites. It is highly likely that the sample has the stoichiometric composition of $SrCrO_2H$. The refined results are summarized in Table 1.

We calculated the Goldschmidt tolerance factor of this perovskite oxyhydride, which is defined by $t = (r_A + r_X) / [\sqrt{2}(r_B + r_X)]$, where r_A , r_B , and r_X denote the ionic radii of the A, B, and X site. Using $r_{Sr^{2+}} = 132$ pm, $r_{Cr^{3+}} = 62$ pm, and $r_X = 140$ pm as employed in many oxides and pure hydrides,^[17] we obtained $t = 1.00$ for $SrCrO_2H$, in agreement with the observed cubic structure. The failure to synthesize $CaCrO_2H$ (not shown) implies that the perfect size matching stabilizes the $SrCrO_2H$ phase. We point out that the aliovalent H^- for O^{2-} substitution allows the use of larger divalent Sr^{2+}

Table 1: Structural parameters of $SrCrO_2H$ from Rietveld refinement of SPXRD (left) and NPD (right) at 300 K.^[a]

Atom	Site	g	x	y	z	U_{iso} (100 Å ²)
Sr^{2+}	1b	1	0.5	0.5	0.5	1.66(4)/1.95(7)
Cr^{3+}	1a	1	0	0	0	0.58(4)/0.86(9)
O^{2-}	3d	0.6699(4)/0.663(2)	0.5	0	0	1.56(9)/1.38(7)
H^-	3d	-/0.337(2)	0.5	0	0	-/1.38(7)

[a] $Pm\bar{3}m$ (no. 221), $a = 3.8344(2)$ Å. $R_{wp} = 8.45\%$, $R_p = 5.44\%$ and $GOF = 3.85$ for SPXRD at room temperature, and $a = 3.8333(1)$ Å. $R_{wp} = 3.85\%$, $R_p = 2.97\%$ and $GOF = 0.96$ for NPD.

cations (versus La^{3+}). This provides access to reach higher t values while preserving the valence of chromium.

The room-temperature NPD data revealed magnetic peaks assigned with (π, π, π) . A magnetic refinement was performed with G -type spin structure. As shown in Figure 2b, we obtained a good fit with a magnetic moment of $1.90 \mu_{\text{B}}$. This observation motivated us to study the temperature evolution of NPD between 25 K and 450 K. The magnetic moment of $2.37(4) \mu_{\text{B}}$ was obtained at the base temperature 25 K, which is slightly smaller than $3 \mu_{\text{B}}$ expected for a Cr^{3+} ion ($d^3, S = 3/2$). Similar values have been indeed reported for Cr^{3+} -containing perovskite oxides, such as LaCrO_3 ($2.45 \mu_{\text{B}}$)^[18] and BiCrO_3 ($2.55 \mu_{\text{B}}$).^[19] Conversely, this fact supports the refined composition of $\text{SrCr}^{3+}\text{O}_2\text{H}$. With increasing temperature, the magnetic peak decreases gradually and finally vanishes at around $T_{\text{N}} \approx 380$ K (Figure 3).

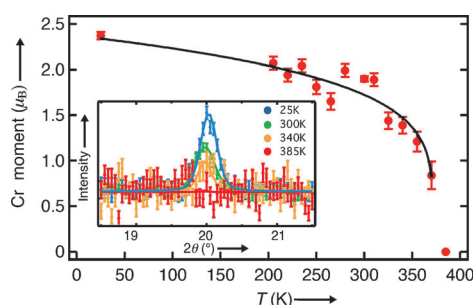


Figure 3. Temperature dependence of the magnetic moment of SrCrO_2H determined by Rietveld refinement of NPD. The solid curve is a guide to the eye. Inset: the normalized $(1/2, 1/2, 1/2)$ magnetic peaks at different temperatures and solid lines represent the Rietveld fit.

SrCrO_2H is a good insulator as in the isoelectric compounds $R\text{Cr}^{3+}\text{O}_3$, where R is a rare earth, thus allowing comparative discussions to be made. The observation of $T_{\text{N}} \approx 380$ K in SrCrO_2H is to our knowledge higher than any chromium oxides (see Table S1 in the Supporting Information). For example, Cr_2O_3 with the corundum structure has $T_{\text{N}} = 307$ K.^[20] In the case of perovskite oxides $R\text{CrO}_3$, the highest T_{N} reported is 290 K in LaCrO_3 .^[21] The significantly higher T_{N} in SrCrO_2H than in $R\text{CrO}_3$ is surprising given that three d electrons in Cr^{3+} (d^3) are in t_{2g} orbitals that cannot overlap with H 1s orbitals (i.e., non-bonding). Although empty e_g orbitals might permit antiferromagnetic spin–spin interactions by a σ -type semi-covalent exchange path, the resultant Cr–H–Cr exchange (J_{H}) should be negligibly small. Thus we suppose that the room-temperature antiferromagnetism of this material is described mainly by the Cr–O–Cr exchange (J_{O}) that allows antiferromagnetic coupling by π -superexchange mechanisms between the Cr half-filled t_{2g} orbitals and the bridging O 2p orbitals.

A high Néel temperature is reported in the layered oxyhydride $\text{LaSrCoO}_3\text{H}_{0.7}$ with $d^{7.3}$ ($T_{\text{N}} = 350$ K). This is because of the presence of electrons in the Co 3d e_g orbital that provides strong σ -type bonds with the H-1s orbital,^[10a,22] a situation completely different from the present material without e_g electrons. What makes the observed T_{N} of SrCrO_2H with four J_{O} bonds (and negligible two J_{H} bonds)

much higher than $R\text{CrO}_3$ with six J_{O} bonds? We suppose that the enhanced magnetic-ordering temperature arises from the relieved octahedral tilting. It is established that $R\text{Cr}^{3+}\text{O}_3$ structures are always considerably distorted from the ideal cubic structure because of relatively small trivalent R cations ($r_{R^{3+}} = 103\text{--}121$ pm).^[23] This leads to smaller t values (below 0.95) and as a result, the CrO_6 octahedra are tilted relative to each other to accommodate the smaller R^{3+} ions. With decreasing t ($R = \text{La} \rightarrow \text{Lu}$), the bending of the Cr–O–Cr increases, leading to weakened J_{O} superexchange interaction and also it enhances the competition between nearest-neighbor (NN) and next-nearest-neighbor (NNN) interactions. As a consequence, the T_{N} of $R\text{CrO}_3$ decreases with decreasing t , as shown in Figure 4. A linear extrapolation of T_{N} toward $t = 1$ yields T_{N} of 460 K in a non-tilted ‘hypo-

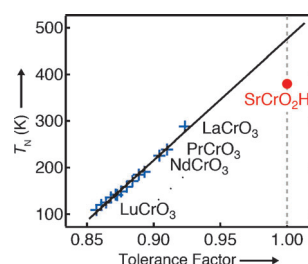


Figure 4. T_{N} values of $R\text{Cr}^{3+}\text{O}_3$ ($R = \text{rare earth}$)^[21] and SrCrO_2H plotted as a function of tolerance factor t .

thetical’ phase of $R\text{CrO}_3$. As the Cr–O–Cr angle approaches the ideal 180° , the orbital overlap integral between Cr 3d t_{2g} and O 2p orbitals is maximized, which should in turn allow for higher T_{N} . Although two J_{O} bonds are lost per Cr in SrCrO_2H , its T_{N} is smaller only by 80 K than the hypothetical cubic $R\text{CrO}_3$. In addition, the Cr–O (Cr–H) distance in SrCrO_2H is 1.917 \AA , which is slightly shorter than the Cr–O distance of approximately 1.98 \AA in $R\text{CrO}_3$ ($R = \text{La–Lu}$). This smaller distance makes J_{O} stronger and contributes to enhance T_{N} .

It is widely accepted that the physical and chemical properties of (layered) perovskite oxides are governed by the tolerance factor. A representative example is manganese perovskite oxides $(R^{3+}_{0.5}A^{2+}_{0.5})\text{MnO}_3$, where electronic phases including ferromagnetic metal and antiferromagnetic insulator are tuned by t .^[1] Such phase control has been mostly achieved by cation (A and/or B) substitution. The present study demonstrates that anion substitution is a useful and highly efficient tool to tune t and obtain improved and new properties. The H-for-O substitution enables a larger ion, Sr^{2+} to be used and permits the 180° angle (while retaining the Cr^{3+} state), so that it is possible to maximize the nearest neighbor J_{O} interactions as well as minimize frustration caused by NN and NNN interactions.

Recent structural studies on oxynitride perovskites ABO_2N ($A = \text{Sr, Ba}$; $B = \text{Ta, Nb}$) have revealed the *cis* preference of BO_4N_2 octahedron, leading to sub-extensive configurational entropies and unusual ‘open order’.^[24] It is related to the correlated order of displacements in ferroelectric perovskites. Although such a *trans* effect may be expected for H^- , our structure is cubic where O^{2-}/H^- ions are apparently disordered. However, if the *cis* preference is achieved (e.g. by varying reaction conditions), SrCrO_2H may

represent a spin analogue of “open order”. Ultimately, a dimensional reduction from three to two will occur in *cis*-constrained ACrOH_2 (A = alkali metal) with disordered zigzag Cr–O–Cr chains arranged within the layers (see Figure S2 in the Supporting Information).

In conclusion, we have successfully synthesized a novel stoichiometric oxyhydride perovskite SrCrO_2H through the use of high-pressure synthesis. SrCrO_2H crystallizes in a cubic perovskite, presumably with disordered O/H arrangement. The most remarkable observation is the occurrence of the antiferromagnetic order as high as 380 K, which is, to our knowledge, the highest among chromium oxides, despite the non-bonding nature of the Cr–H–Cr interaction. The high T_N value is explained by the relieved octahedral tilting that enhances the Cr–O–Cr antiferromagnetic coupling and the reduced frustration between nearest neighbor and next-nearest neighbor interactions. In SrCrO_2H , the lack of e_g electrons results in a frontier orbital symmetry of H^- (σ) that is different from those of other anions O^{2-} , N^{3-} , F^- (σ , π). It would be exciting to prepare, for example, $\text{Sr}_{1-x}\text{La}_x\text{CrO}_{2-x}\text{H}_x$ and $\text{SrCrO}_{2-x}\text{H}_x$, to continuously modify the tilting angles, carrier concentration, and magnetic interaction to develop novel anion-controlled properties.

Experimental Section

A polycrystalline SrCrO_2H sample was synthesized by solid-state reaction at high pressure and elevated temperature using a cubic anvil high-pressure apparatus. SrO (99.99%, Aldrich), and Cr_2O_3 (99.9%, Kojundo), and laboratory prepared SrH_2 were used as starting reagents. The appropriate amounts of starting reagents were mixed thoroughly in an agate mortar in the glovebox. The mixed sample was charged into a NaCl sleeve as a pressure-transmitting medium inside a graphite heater. The pressure applied ranges 4–8 GPa and the sample was heated at 5 K min^{-1} under O_2 flow and gaseous products were monitored simultaneously. TEM data was collected at room temperature with a JEM 1400 microscope (JEOL). SPXRD experiments were performed on a Debye–Scherrer camera at the BL02B2 beamline at SPring-8. The NPD data for refinement were collected between 25 K and 385 K using a Cu311 monochromator ($\lambda = 1.5401\text{ \AA}$) at NIST Center for Neutron Research. The temperature evolution was also studied at the WOMBAT diffractometer of the Bragg Institute at ANSTO. Structural refinements were carried out using JANA2006.^[25] EDS was collected by an Oxford x-act detector mounted on a Hitachi S-3400N SEM.

Received: May 20, 2014

Published online: August 12, 2014

Keywords: chromium · high-pressure chemistry · mixed anion phases · oxyhydrides · perovskites

- [2] C. Dubourdieu, J. Bruley, T. M. Arruda, A. Posadas, J. Jordan-Sweet, M. M. Frank, E. Cartier, D. J. Frank, S. V. Kalinin, A. A. Demkov, V. Narayanan, *Nat. Nanotechnol.* **2013**, *8*, 748.
- [3] R. J. Cava, B. Batlogg, J. J. Krajewski, R. Farrow, L. W. Rupp, A. E. White, K. Short, W. F. Peck, T. Kometani, *Nature* **1988**, *332*, 814.
- [4] M. Jansen, H. P. Letschert, *Nature* **2000**, *404*, 980.
- [5] A. Kasahara, K. Nukumizu, G. Hitoki, T. Takata, J. N. Kondo, M. Hara, H. Kobayashi, K. Domen, *J. Phys. Chem. A* **2002**, *106*, 6750.
- [6] a) Y.-I. Kim, P. M. Woodward, K. Z. Baba-Kishi, C. W. Tai, *Chem. Mater.* **2004**, *16*, 1267; b) Y.-R. Zhang, T. Motohashi, Y. Masubuchi, S. Kikkawa, *J. Eur. Ceram. Soc.* **2012**, *32*, 1269.
- [7] W. Tong, W. S. Yoon, N. M. Hagh, G. G. Amatucci, *Chem. Mater.* **2009**, *21*, 2139.
- [8] a) B. Malaman, J. F. Brice, *J. Solid State Chem.* **1984**, *53*, 44; b) B. Huang, J. D. Corbett, *Inorg. Chem.* **1998**, *37*, 1892.
- [9] S. Iimura, S. Matsushita, H. Sato, T. Hanna, Y. Muraba, S. W. Kim, J. E. Kim, M. Takata, H. Hosono, *Nat. Commun.* **2012**, *3*, 943.
- [10] a) M. A. Hayward, E. J. Cussen, J. B. Claridge, M. Bieringer, M. J. Rosseinsky, C. J. Kiely, S. J. Blundell, I. M. Marshall, F. L. Pratt, *Science* **2002**, *295*, 1882; b) R. M. Helps, N. H. Rees, M. A. Hayward, *Inorg. Chem.* **2010**, *49*, 11062.
- [11] Y. Kobayashi, O. J. Hernandez, T. Sakaguchi, T. Yajima, T. Roisnel, Y. Tsujimoto, M. Morita, Y. Noda, Y. Mogami, A. Kitada, M. Ohkura, S. Hosokawa, Z. Li, K. Hayashi, Y. Kusano, J. E. Kim, N. Tsuji, A. Fujiwara, Y. Matsushita, K. Yoshimura, K. Takegoshi, M. Inoue, M. Takano, H. Kageyama, *Nat. Mater.* **2012**, *11*, 507.
- [12] a) Y. Tsujimoto, C. Tassel, N. Hayashi, T. Watanabe, H. Kageyama, K. Yoshimura, M. Takano, M. Ceretti, C. Ritter, W. Paulus, *Nature* **2007**, *450*, 1062; b) M. A. Hayward, M. A. Green, M. J. Rosseinsky, J. Sloan, *J. Am. Chem. Soc.* **1999**, *121*, 8843.
- [13] a) J. V. Badding, R. J. Hemley, H. K. Mao, *Science* **1991**, *253*, 421; b) S. Ayukawa, K. Ikeda, M. Kato, T. Noji, S. Orimo, Y. Koike, *J. Phys. Soc. Jpn.* **2012**, *81*, 034704; c) R. Sato, H. Saitoh, N. Endo, S. Takagi, M. Matsuo, K. Aoki, S. Orimo, *Appl. Phys. Lett.* **2013**, *102*, 091901.
- [14] V. Peres, L. Favergeon, M. Andrieu, J. C. Palussière, J. Balland, C. Delafay, M. Pijolat, *J. Nucl. Mater.* **2012**, *423*, 93.
- [15] A. M. Arévalo-López, J. A. Rodgers, M. S. Senn, F. Sher, J. Farnham, W. Gibbs, J. P. Attfield, *Angew. Chem.* **2012**, *124*, 10949; *Angew. Chem. Int. Ed.* **2012**, *51*, 10791.
- [16] B. L. Chamberland, *Solid State Commun.* **1967**, *5*, 663.
- [17] K. Ikeda, Y. Nakamori, S. Orimo, *Acta Mater.* **2005**, *53*, 3453.
- [18] E. F. Bertaut, G. Bassi, G. Buisson, P. Burlet, J. Chappert, A. Delapalme, J. Mareschal, G. Roult, R. Aleonard, R. Pauthenet, J. P. Rebouillat, *J. Appl. Phys.* **1966**, *37*, 1038.
- [19] A. A. Belik, S. Iikubo, K. Kodama, N. Igawa, S. Shamoto, E. Takayama-Muromachi, *Chem. Mater.* **2008**, *20*, 3765.
- [20] a) T. R. McGuire, E. J. Scott, F. H. Grannis, *Phys. Rev. Lett.* **1956**, *102*, 1000; b) A. Iyama, T. Kimura, *Phys. Rev. B* **2013**, *87*, 180408(R).
- [21] a) R. Aleonard, R. Pauthenet, J. P. Rebouillat, C. Veyret, *J. Appl. Phys.* **1968**, *39*, 379; b) I. Weinberg, P. Larssen, *Nature* **1961**, *192*, 445.
- [22] S. J. Blundell, I. M. Marshall, F. L. Pratt, M. A. Hayward, E. J. Cussen, J. B. Claridge, M. Bieringer, C. J. Kiely, M. J. Rosseinsky, *Physica B* **2003**, *326*, 527.
- [23] a) R. D. Shannon, *Acta Crystallogr. Sect. A* **1976**, *32*, 751; b) R. D. Shannon, C. T. Prewitt, *Acta Crystallogr. Sect. B* **1969**, *25*, 925.
- [24] M. Yang, J. Oró-Solé, J. A. Rodgers, A. Belén Jorge, A. Fuertes, J. P. Attfield, *Nat. Chem.* **2011**, *3*, 47.
- [25] V. Petricek, M. Dusek, L. Palatinus, *Z. Kristallogr.* **2014**, *229*(5), 345.

[1] C. N. R. Rao, B. Raveau, *Colossal Magnetoresistance, Charge Ordering and Related Properties of Manganese Oxides*, World Scientific, Singapore, **1998**.